



**HAL**  
open science

## Experimental Investigation of Repetitive Femtosecond Laser Energy Deposition in a M=3 Supersonic Airflow

Paul-Quentin Elias, Benjamin Khiar, Sylvain Morilhat, Nicolas Severac, Jean-Marc Luysen, Jean-Pierre Tobeli, Reynald Bur, Ivan Doudet, Benoit Wattelier, Laurent Bizet, et al.

► **To cite this version:**

Paul-Quentin Elias, Benjamin Khiar, Sylvain Morilhat, Nicolas Severac, Jean-Marc Luysen, et al.. Experimental Investigation of Repetitive Femtosecond Laser Energy Deposition in a M=3 Supersonic Airflow. AIAA ScieTech 2024 Forum, AIAA, Jan 2024, Orlando, United States. pp.1651, 10.2514/6.2024-1651 . hal-04382938

**HAL Id: hal-04382938**

**<https://hal.science/hal-04382938v1>**

Submitted on 17 Oct 2024

**HAL** is a multi-disciplinary open access archive for the deposit and dissemination of scientific research documents, whether they are published or not. The documents may come from teaching and research institutions in France or abroad, or from public or private research centers.

L'archive ouverte pluridisciplinaire **HAL**, est destinée au dépôt et à la diffusion de documents scientifiques de niveau recherche, publiés ou non, émanant des établissements d'enseignement et de recherche français ou étrangers, des laboratoires publics ou privés.

# Experimental Investigation of Repetitive Femtosecond Laser Energy deposition in a M=3 Supersonic Airflow

P.-Q. Elias and B. Khiar

*DPHY, ONERA, Université Paris Saclay F-91123 Palaiseau -France*

S. Morilhat, N. Severac, J.-M. Luysen, J.-P. Tobeli, R. Bur

*DAAA, ONERA, Université Paris Saclay F-92190, Meudon – France*

I. Doudet, B. Wattellier

*Phasics, Saint-Aubin ,F-91190, France*

L. Bizet, Y.-B. André, B. Mahieu, A. Mysyrowicz, A. Houard

*Laboratoire d'Optique Appliquée – ENSTA Paris - École Polytechnique, CNRS IP Paris, Palaiseau, F-91761, France*

**A picosecond 200-mJ pulsed laser operating at 1 kHz is used to create large aspect ratio heated channels in front of a blunted test model in a M=3 flow. The energy deposition induces a significant disturbance of the flow and large fluctuations of the drag signal. The heated region extends over 50-80 mm upstream of the test item. For this given repetition rate, the raw drag balance signal shows no significant decrease in the averaged drag, which could be due to the vibration induced by the fluctuating drag on the mechanical system.**

## I. Introduction

The deposition of energy upstream of a supersonic body can induce significant disturbances in the flow. This method is appealing for several applications, such as drag reduction, flow control or sonic boom alleviation. Off-body energy deposition is mediated by the generation of a plasma which is formed through two methods: focused microwave breakdown [1] or laser-induced breakdown [2]. In the latter case, when the laser power exceeds a threshold depending on the incoming flow properties (nature of the gas, density, etc.), the gas breakdown leads to the formation of a plasma. When the laser pulse duration is in the nanosecond range, the plasma kernel consists in a small volume of a few cubic millimeters. When the pulse duration is in the femtosecond range, lasers can form long plasma filaments over distances ranging from several centimeters to several meters [3]. Depending on the pulse energy, the filament can induce a significant heating of the gas [4] which can be used advantageously for high speed flow control, in particular for drag reduction. This idea has been demonstrated experimentally using a femtosecond laser in single pulse mode, delivering a pulse energy around 200 mJ [5], [6]. While the effect of single pulse can lead to a transient drag reduction above 40%, a quasi-steady effect on the flow requires a repetitive action. More precisely, for an energy deposition of length  $L$  ( $\sim 50$  mm in [6]) in an airflow of velocity  $U_0$  ( $\sim 600$  m/s), experiments have shown that the total duration of the interaction is  $\tau \sim 4L/U_0$ . Therefore, the critical repetition rate above which quasi-steady effects appear scales as  $1/\tau$ , typically several kilohertz with the previous parameters. Femtosecond/ picosecond lasers with pulse energy large enough ( $> 100$  mJ) operating in this repetition rate range are very few. Recently, in the frame of the Laser Lightning Rod project, such a laser, operating at 1 kHz, was developed to successfully guide a lightning strike [7]. The goal of this study is to use this laser in repetitive mode to demonstrate near quasi-steady drag reduction on a supersonic body.

## II. Test setup

### A. Supersonic wind-tunnel

The test facility used was ONERA's R1Ch blow-down supersonic wind tunnel fitted with a  $M = 3$  nozzle (mass flow  $\sim 15\text{-}18$  kg/s depending on the stagnation pressure, nozzle exit section diameter of 310 mm). The test item was mounted in front of the nozzle exit section. In this facility, the supersonic airflow decelerates downstream of the model in a supersonic diffuser which is connected to a vacuum sphere ( $500\text{ m}^3$ ). The tests runs duration is between 10 and 25s, depending on the operation parameters. For this experiment, stagnation pressures ranging between 2.5 and 4.5 bar were considered. The stagnation temperature was in the range [280-290K]. Under these conditions, the freestream unit Reynolds number was between  $2 \times 10^7\text{ m}^{-1}$  and  $3.6 \times 10^7\text{ m}^{-1}$ . The run duration was set to 10s.

The wind tunnel chamber is fitted with two rectangular windows (400x300 mm) for the optical diagnostics and several feedthroughs which can be fitted with optical windows to inject the laser in the chamber.

### B. Laser & optical setup

The LLR laser system used in this experiment was initially developed for atmospheric research. In its nominal configuration, it is composed of several main components:

- A seed laser operating at 1 kHz and 1030 nm,
- a regenerative amplifier which amplifies the seed pulse energy to approximately 240 mJ,
- an innovative multipass amplifier that further increase the pulse energy to 800 mJ
- a compressor to bring the pulse duration to 1 ps with a slight decrease of the energy (720mJ)

Due to size constraint next to the wind tunnel, the multipass amplifier was not used. The output of the regenerative amplifier was directly fed to the compressor. In these conditions, the resulting pulse energy was 200 mJ, for a pulse duration of 1 picosecond and a repetition rate of 1 kHz. The laser system is 5 meters long and 1.4 m wide. To insure a dust free environment, it is enclosed in a tent fitted with laminar air-flux filter. A detailed description of the laser system can be found in [8].

The maximum laser pulse energy, measured at the laser output with a powermeter, was  $E = 207$  mJ, giving an averaged laser power of 200 W. The laser beam was guided in the wind tunnel chamber using a periscope (75 mm mirror with an anti-reflection coating for 1030 nm and 515 nm). The beam entered the chamber through a laser-grade silica window (70 mm in diameter, 6 mm in width, anti-reflection coating for 1030 and 515 nm). Before being injected in the test model, the beam was focused by a converging lens (focal length 1000 mm). The focal point was located approximately 80 mm upstream of the test model, along the model axis.

### C. Test Item

The test item was a modified normalized blunt body (HB1, see [8], 60 mm in diameter), as shown in Figure 1. It was identical to the one used in a previous study with a different femtosecond laser [6]. Whereas the length of the cylindrical part of the normalized HB1 profile is  $4.083D$ , where  $D$  is the main diameter, the length of the cylindrical part of our model was  $0.88D$ . The reason for this modification was to maintain a distance between the nozzle exit section and the test model large enough to have a side view of the laser filament. In addition, the need to keep the whole model in the Mach rhombus of the nozzle in order to avoid velocity and density gradients of the flow constrained the position and size of the test item.

The model was hollowed to enable the internal propagation of the laser beam, as shown in Figure 2. The stagnation point of the model had a 3-mm diaphragm through which passes the converging beam.

The truncated cone was manufactured in PEEK. The cylindrical part of the model was made of an aluminum sleeve. A holding sting connected the model and its balance to the supporting table. The support was adjusted to have zero pitch and yaw angles with respect to the flow direction, as given by the nozzle axis.

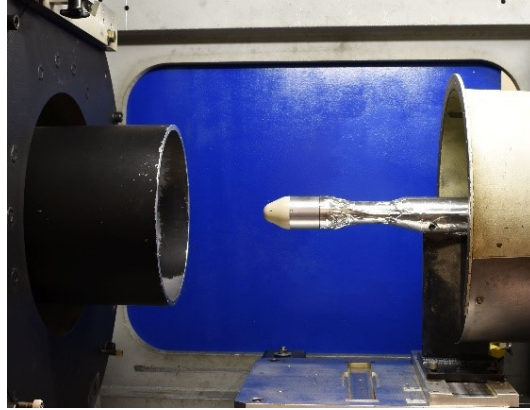


Figure 1. Side view of the test item in the R1Ch wind tunnel.

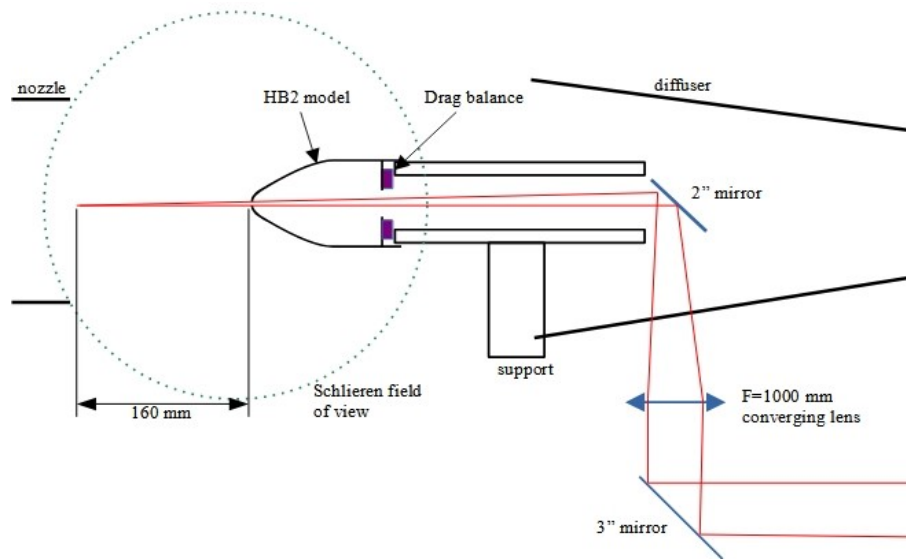


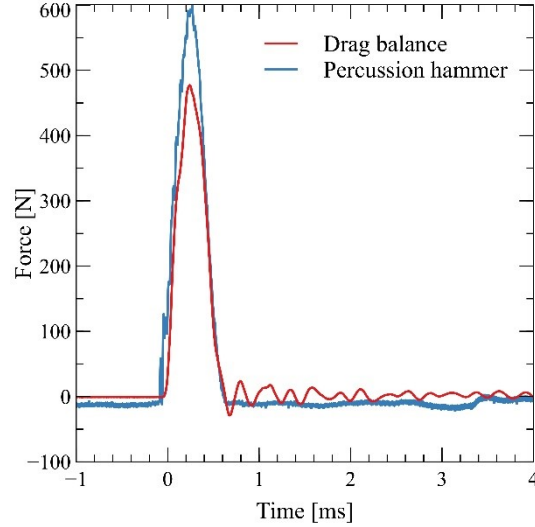
Figure 2. Schematic view of the laser injection path.

## D. Diagnostics

### 1. Drag balance

The drag balance included a weighted plate that held the test model and a fixed plate mounted on the holding sting. The drag force was measured with three prestressed piezoelectric Kistler force sensors (type 9134B) mounted at  $120^\circ$  around the model axis, between these two plates. These sensors measured the axial component of the drag. The sensor outputs were connected in parallel to a Kistler 5018 amplifier.

The response of the balance was checked with a percussion hammer (Bruel & Kjaer Type 8202) fitted with a steel tip to have the shortest excitation. The nose of the model was hit with the hammer and the response of the hammer accelerometer and the drag balance signal were recorded. A typical view of this signal is shown in Figure 3. The balance is able to resolve 600- $\mu$ s wide impulses. There is a slight ringing of the balance after the impulse.



**Figure 3. Force measured by the drag balance and the percussion hammer, for a strike applied on the test model nose.**

### 2. Schlieren system

A Z-type Schlieren system was used to visualize the flow features. It was composed of two 300-mm parabolic mirrors (focal length 1100 mm) located on either side of the test chamber. The emission side used a Cavilux Smart pulsed laser as a light source. The laser output from the optic fiber was focused with a condenser ( $F = 75$  mm) to a knife located at the focal point of the mirror. The collimated beam passed through the test chamber through two rectangular windows (thickness 54 mm) to reach the second parabolic mirror. A second knife was located in the second mirror focal plane. The test model was imaged with a 150 mm converging lens and a camera lens (F200) on a Phantom V2640 high-speed camera.

The high-speed camera ran at 28,000 frames per second. Its strobe signal triggered the pulsed laser source. The camera exposure time was set to 1  $\mu$ s. The laser pulse duration was set to 100 ns.

### 3. Acquisition system

The main signals of the experiments were the following:

- The output of the drag balance amplifier, which is proportional to the drag force;
- A photodiode signal used to detect the laser pulse. Note that the photodiode response integrates the 1-ps pulse. Its typical output is a pulse with a  $\sim 10$ -20 ns rise time and  $\sim 1$   $\mu$ s decay time;
- The strobe signal of the high-speed camera, used to synchronize the camera's frames.

These signals were recorded on a digital acquisition system (NIDAQ PXie6376, 16 bits). The acquisition frequency was set to  $2.5 \times 10^6$  samples per second. During the run, 50 buffers of 250,000 points (duration 100 ms) were recorded every 500 ms. A delay generator triggered the DAQ and the high-speed camera. The delay between the timing and the acquisition system is less than 0.1  $\mu$ s

## III. Results

### A. Test conditions

The baseline test conditions for the experiments are given in Table 1. Variations of the stagnation pressure between 2.5 bar and 4.5 bar were also tested.

The LLR laser system needs approximately 5 seconds to reach its target power. With the wind tunnel runtime of 10 seconds, it was not possible to cycle on and off the laser during the run. Therefore, the laser was started 5 seconds prior to the run. During this period, the chamber was at the same pressure as the vacuum sphere (a few millibars) and no plasma filament was observed. After the beginning of the flow, the laser was left running for approximately 5 seconds and then switched off to reach zero power at the end of the run. This cutoff prior to the end of the run was

required to avoid damaging the rear mirror during the cutoff. In fact, when the run ends, the closure of a downstream gate valve induces large overpressure on the test models. These pressure variations were found to perturb significantly the laser propagation to the point of leading to damages on the optical surface of the mirror.

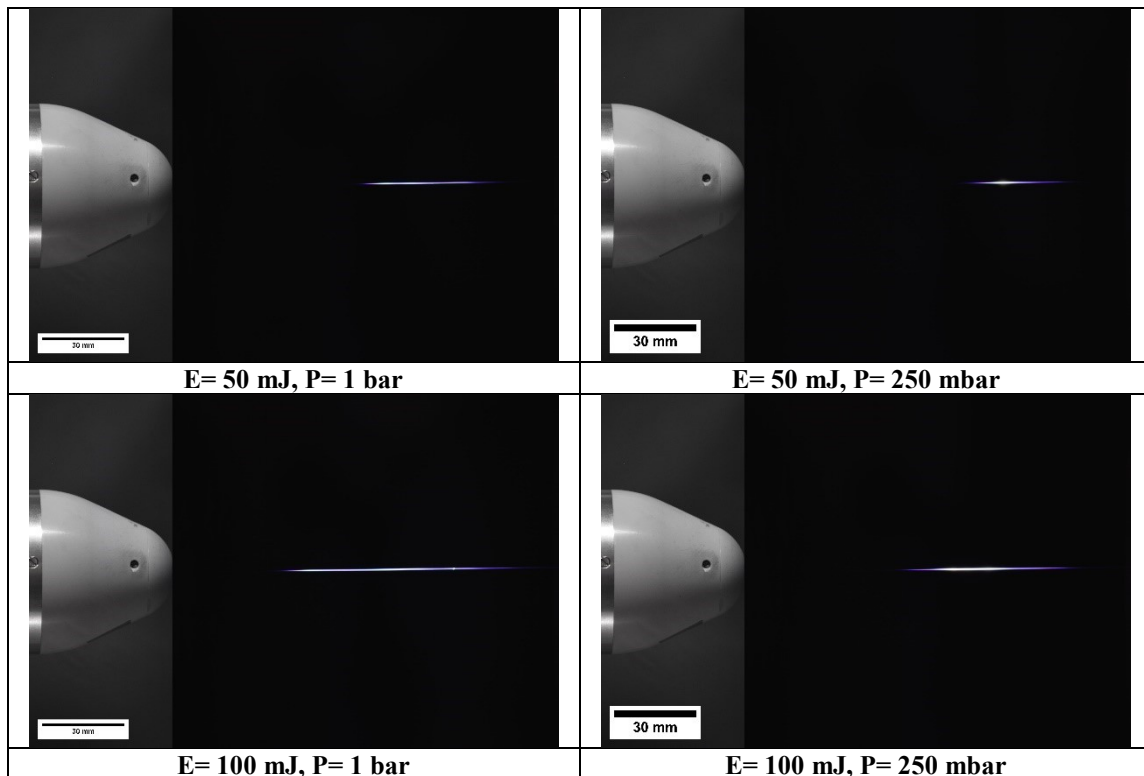
**Table 1- Typical flow conditions.**

Mach number	3,0
Stagnation Pressure (Pa)	$3.6 \times 10^5$
Stagnation Temperature (K)	283 +/-3
Freestream pressure (Pa)	9 800 +/- 50
Freestream temperature (K)	102
Freestream gas density ( $\text{kg. m}^{-3}$ )	0.33
Freestream flow velocity ( $\text{m.s}^{-1}$ )	604 +/- 4
Freestream unit Reynolds ( $\text{m}^{-1}$ )	$2.9 \times 10^7$
Focal point distance from nose (mm)	154 +/- 5
Laser wavelength (nm)	1030
Laser repetition rate (Hz)	1003.8

## B. Observations

### 1. Quiescent air

Figure 4 shows the emission from the plasma filament obtained in quiescent air at atmospheric pressure and at 250 mbar. At this latter pressure, the gas density is  $\sim 0.3 \text{ kg.m}^{-3}$ , close the freestream gas density during the experiments. The extent of the luminous zone correlates with size of the plasma formed by the filament. At lower pressure, the filaments are shorter, as expected for sub-picosecond filamentation in air[9]. Assuming that the emissive zone gives the extent of the heated volume, we can use the image intensity to estimate its length. The width at half maximum is around 80 mm for the maximum pulse energy.



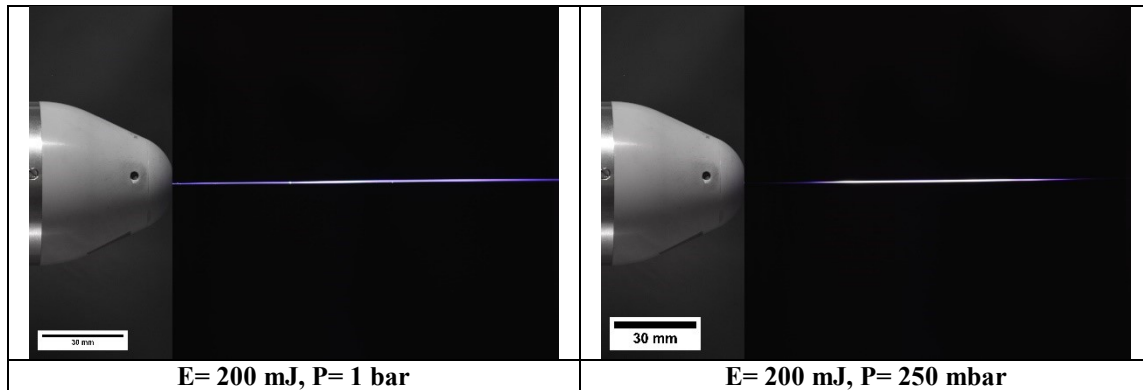


Figure 4. View of the plasma filament in quiescent air, for different pulse energies and pressures (exposure time 1 second).

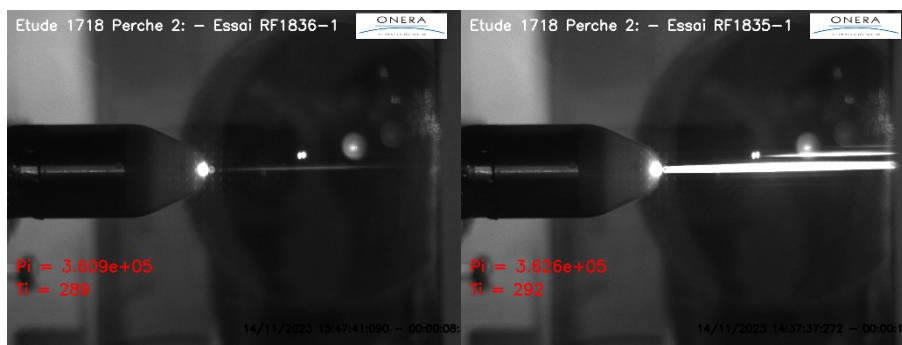


Figure 5. View of the filaments during run 1836 (left) and run 1835 (right). A sharp increase of the filament emission is observed during run 1835. The flow parameters ( $P_{st} = 3.5$  bar) and laser parameters ( $E = 200$  mJ) are the same in both cases.

## 2. Supersonic flow

When the laser was activated in the airflow, we observed the formation of a luminous zone upstream of the test model, as shown in Figure 5. The schlieren images show the formation, the convection and the interaction with the bow shock of an elongated heated volume, as seen in Figure 6. The phenomenology of this interaction is consistent with the results obtained previously with numerical simulations or experiments with a low repetition rate femtosecond laser[6]

In some instances, the intensity of this zone appeared much higher, as shown in Figure 5. This increased intensity was observed several times but its origin is not understood. It could be due to the sensitivity of the filament generation to the laser alignment as the beam passes through the test model. Another hypothesis is the presence of dust in the flow, which might enhance the filamentation. In that case, we observed that the heated volume produced by the laser filament is longer and broader, as shown in Figure 7. The phenomenology of the interaction is identical, but the recirculating bubble formed by the convection of the heated column is broader and longer.

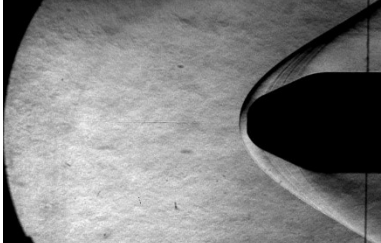

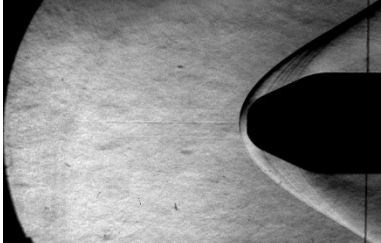
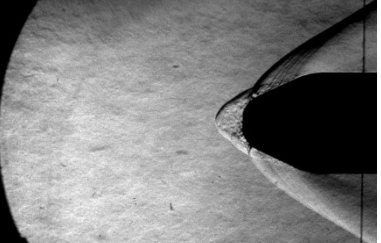
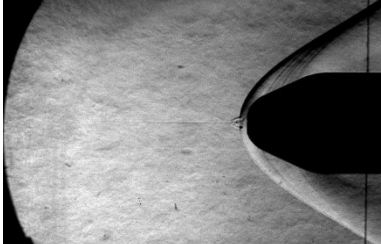
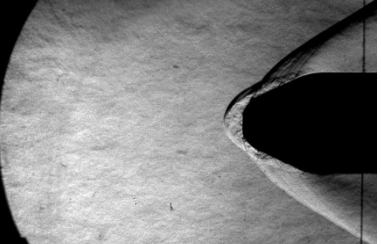
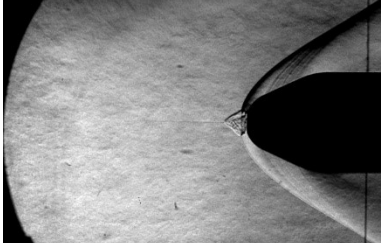
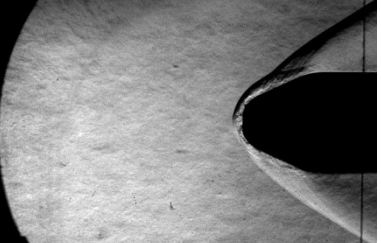
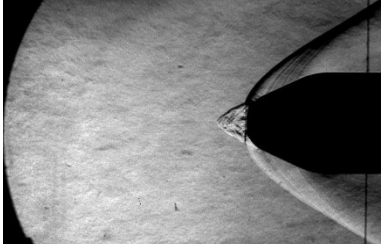
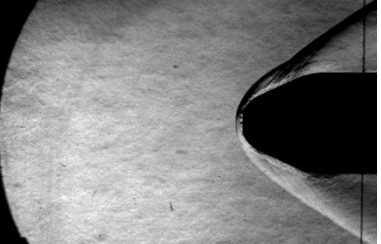
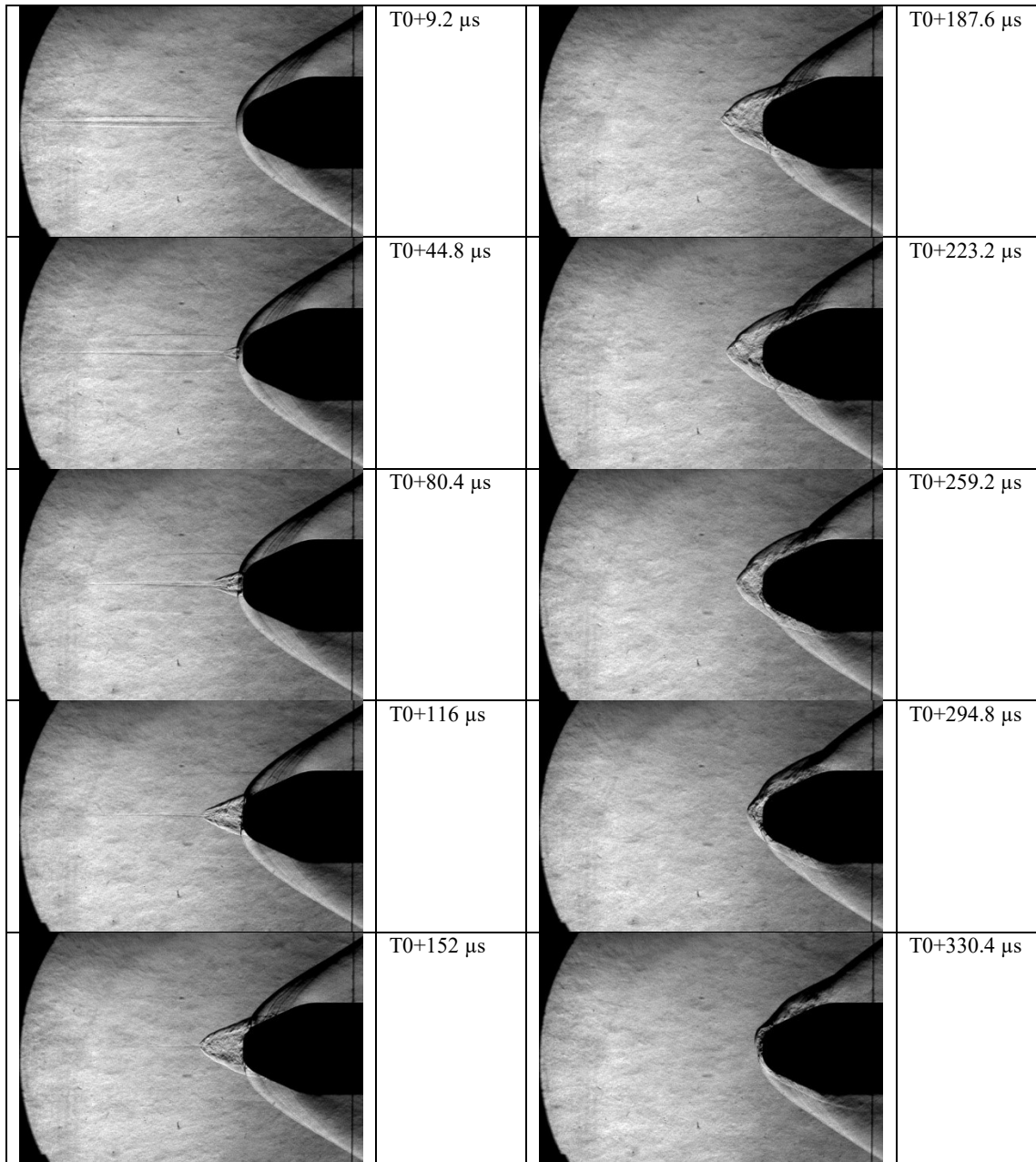
	T0+0.8 μs		T0+179.6 μs
	T0+36.8 μs		T0+215.2 μs
	T0+72.4 μs		T0+250.8 μs
	T0+108 μs		T0+286.8 μs
	T0+143.6 μs		T0+322.4 μs

Figure 6. Time evolution of the flow after the energy deposition (T0), run 1836.



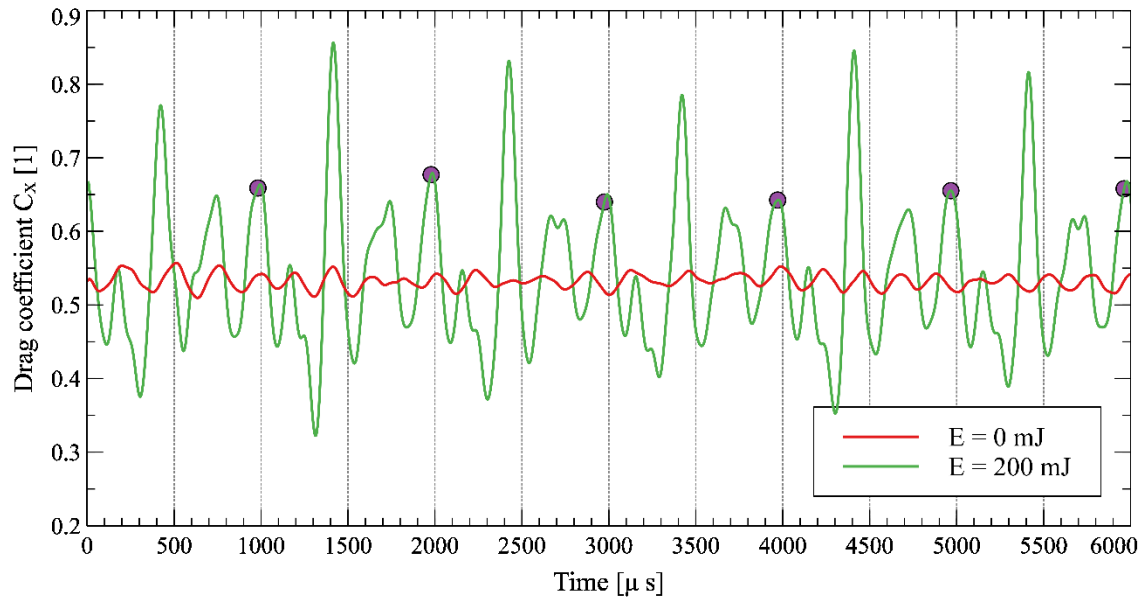


**Figure 7. Time evolution of the flow after the energy deposition (T0), run 1835.**

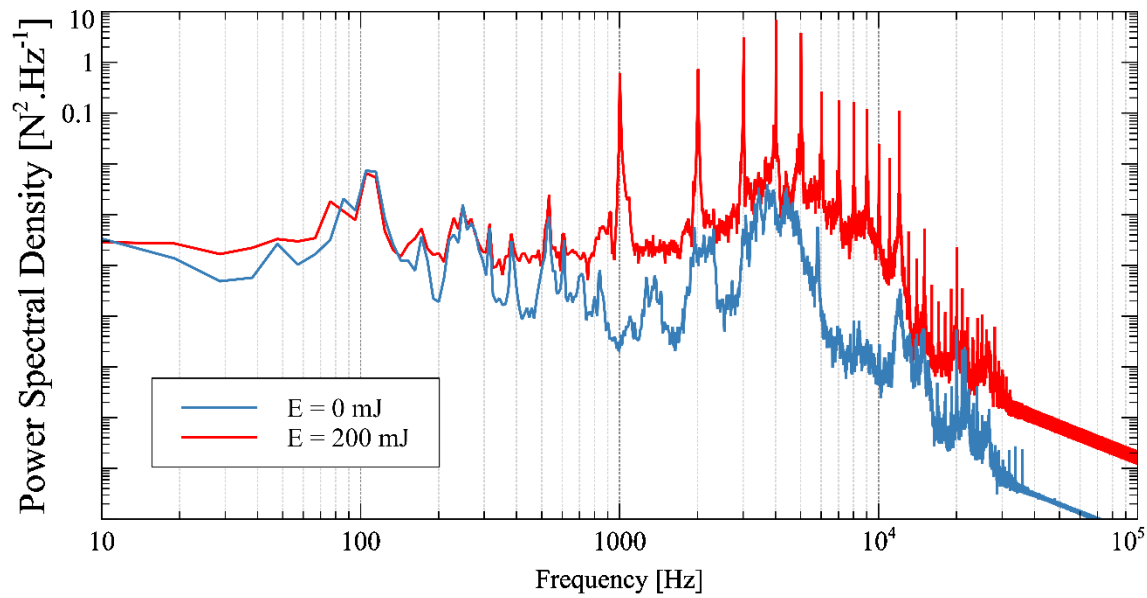
### C. Drag measurements

An example of the time evolution of the drag coefficient is shown in Figure 8. When the laser was activated, we observed large oscillation in the drag coefficient. The repetitive activation of the laser (every 1 ms) causes repetitive changes in the drag force applied to the test model. Based on previous results and on the schlieren images, we can assume that the drag variation lasts for approximately 300 μs. Thus, the duty cycle of the excitation was around 30%. This repetitive force on the balance excites the mechanical structure formed by the test model and the balance assembly, which responds with a quasi-periodic signal. Approximately 300 μs after the laser pulse, we notice a drop in the drag (30-40% reduction), followed by a significant overshoot (50-60% increases). This behavior is also consistent with what has been previously observed for single shot laser pulses.

A comparison of the power spectral density of the drag signal with and without laser is shown in Figure 9. The main frequency of the laser and its harmonics appears clearly as peaks at least two orders of magnitude more intense than the balance baseline response.

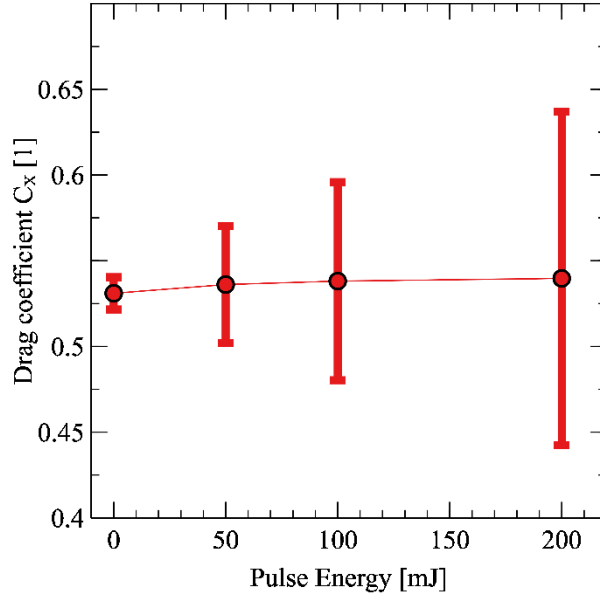


**Figure 8.** Time evolution of the drag coefficient with the laser on (Run 1825, Trun + 3s, 200 mJ) and with the laser off (Run 1832, Trun+3s, 0 mJ). The arrival times of the laser pulses are shown by the purple circles.



**Figure 9.** Power spectral density of the drag signal, for two cases (Run 1825: E = 200 mJ and Run 1832: E = 0 mJ).

In Figure 10, we plot the mean drag coefficient versus laser pulse energy. The error bars give the standard deviations of the drag. The higher the pulse energy is (or equivalently, the average power), the higher the drag fluctuations. The averaged drag remains nearly constant, with a slight increase (less the 2%) when the laser is on.



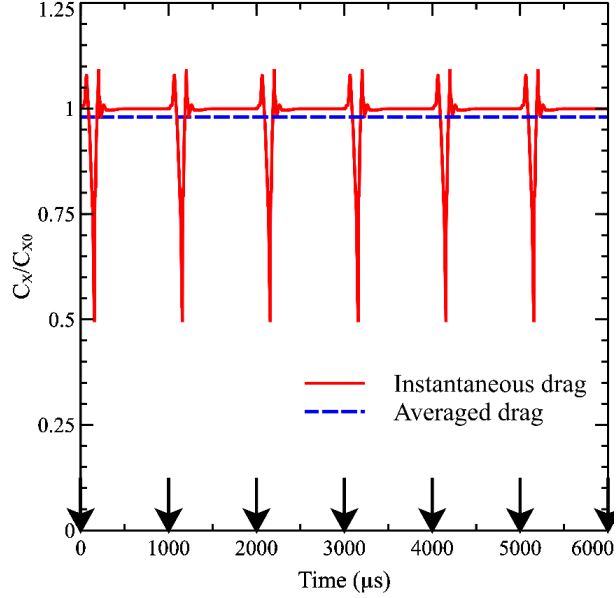
**Figure 10. Mean drag coefficient as a function of laser pulse energy. The error bars are given by the drag signal standard deviation. (Runs 1832, 1818, 1817, 1825, by increasing pulse energy)**

#### IV. Discussion

The later point is worth discussing, as we would expect a decrease of the mean drag with the repetitive laser energy deposition. Indeed, using numerical results obtained previously, it is possible to estimate the drag force variations experienced by the model, as shown in Figure 11. In that case, the time-averaged drag is expected to decrease by 2.5 %. This is not what was observed in our experiments. The averaged drag remains nearly constant or slightly increasing. Several factors could explain this fact:

1. Balance+ Test model non-linearity: The drag signal seen in Figure 8 is puzzling because of the large overshoot of the drag signal. After the laser pulse arrival, the balance signal decreases due to the drop of the drag. However, the recovery phase, which is expected in such a mechanical system, shows a large overshoot. In a linear mechanical system (with dissipation), the overshoot magnitude cannot exceed the magnitude of the initial drag dip. However, in our case, the aerodynamic force already stresses the test models. The non-linear release of this stress during the recovery phase could explain this large overshoot.

2. Compound effect : The test-model balance assembly can be roughly seen as a mass-spring system. However, the sting holding the base plate of the balance could also be seen as a mass spring system. In this simple picture, we have two serial mass-spring systems. The variation of the drag could induce out-of-phase displacement of the masses. If the heavier sting keeps expanding as the lighter test model is already pushed back by the recovery of the flow, the stress on the balance could overshoot the linear response. Note that this phenomenon is not exclusive of the previous one.



**Figure 11. Instantaneous drag variation from the repetitive laser energy deposition ( $f=1$  kHz). The drag variations are given by previous numerical simulations [6]. The dashed line show the averaged drag. The laser pulse arrival times are shown by the black arrows.**

## V. Conclusion

In this work, we have studied the effect of repetitive laser energy deposition on the flow around a blunted cone. Using a picosecond laser with a maximum pulse energy of 200 mJ and a repetition rate of 1 kHz, the laser energy deposition operates in the filamentation regime, characterized by the formation of an elongated ( $\sim 50$ -80 mm) heated channel in front of the model nose. The axial extent of the heated channel increases as the pulse energy increases.

The flow features observed during the repetitive laser pulses are consistent with previous ones in single shot mode. However, the repetition rate of the pulsed induces a strong mechanical excitation of the model, which was not previously seen. The excitation amplitude is correlated to laser pulse energy. We do not measure any significant effect on the mean drag, but this could be due to the mechanical response of the balance assembly, which screens the effect of the laser deposition.

Future work will focus on four topics:

1. Increase of the laser repetition rate to 5 kHz: at 1 kHz, for 200 mJ pulses, we obtained heated column of length 50-80 mm. In that case, we observed that the interaction with the shock systems lasts for approximately 300  $\mu$ s. The LLR laser can be tuned to operate at higher frequency, the average power being constant. If the laser pulse period is smaller than the interaction duration, we can expect a nearly steady effect of the energy deposition. The drawback is that the increase in frequency translates in a pulse energy reduced to 30-40 mJ, giving a shorter heated channel.
2. Finer modeling of the mechanical response of the balance: When it is operated at 1 kHz, the laser continuously excites mechanical modes of the model + balance assembly. This frequency is not far from the resonance frequency (around 4 kHz). By modeling the balance as a series of dampened mass-spring systems, we intend to replicate the mechanical response of the balance to estimate the effect of the flow perturbations.
3. Measurement of the heated channel density profile: It has been shown previously that repetitive laser filaments form a low-density heated channel [10]. In the supersonic flow, the convective time is smaller than the repetition period. Therefore, each filament is formed in unperturbed air. Using a wavefront sensor [6], we will measure the density profile of the filament in the freestream. This measurement will be useful to characterize the heated channel and will help in tuning the numerical simulations of the interactions.
4. Off-axis laser injection: This work considered a laser injection along the symmetry axis of the test item, to measure its effect on the drag. We will also investigate off-axis laser energy deposition and its possible use to generate lateral efforts.

## Acknowledgments

The authors acknowledge the financial support of the ANR (Agence National Pour la Recherche) and AID (Agence Innovation Défense) through the ANR ASTRID grant ANR-20-ASTR-0015-1

## References

- [1] V. Lashkov, I. Mashek, Y. Anisimov, V. Ivanov, Y. Kolesnichenko, et M. Ryvkin, « Gas Dynamic Effect of Microwave Discharge on Supersonic Cone-shaped Bodies », in *42nd AIAA Aerospace Sciences Meeting and Exhibit*, in Aerospace Sciences Meetings. , American Institute of Aeronautics and Astronautics, 2004. doi: 10.2514/6.2004-671.
- [2] D. Knight et N. Kianvashrad, « Review of Energy Deposition for High-Speed Flow Control », *Energies*, vol. 15, n° 24, Art. n° 24, janv. 2022, doi: 10.3390/en15249645.
- [3] A. Couairon et A. Mysyrowicz, « Femtosecond filamentation in transparent media », *Physics Reports*, vol. 441, n° 2, p. 47-189, mars 2007, doi: 10.1016/j.physrep.2006.12.005.
- [4] G. Point *et al.*, « Superfilamentation in Air », *Phys. Rev. Lett.*, vol. 112, n° 22, p. 223902, juin 2014, doi: 10.1103/PhysRevLett.112.223902.
- [5] P.-Q. Elias, « Numerical Simulations on the Effect and Efficiency of Long Linear Energy Deposition Ahead of a Supersonic Blunt Body: Toward a Laser Spike », *AerospaceLab Journal*, vol. Issue 10, p. 11 pages, 2015, doi: 10.12762/2015.AL10-03.
- [6] P.-Q. Elias *et al.*, « Improving supersonic flights with femtosecond laser filamentation », *Sci. Adv.*, vol. 4, n° 11, p. eaau5239, nov. 2018, doi: 10.1126/sciadv.aau5239.
- [7] A. Houard *et al.*, « Laser-guided lightning », *Nat. Photon.*, p. 1-5, janv. 2023, doi: 10.1038/s41566-022-01139-z.
- [8] C. Herkommer *et al.*, « Ultrafast thin-disk multipass amplifier with 720 mJ operating at kilohertz repetition rate for applications in atmospheric research », *Opt. Express, OE*, vol. 28, n° 20, p. 30164-30173, sept. 2020, doi: 10.1364/OE.404185.
- [9] G. Méchain, T. Olivier, M. Franco, A. Couairon, B. Prade, et A. Mysyrowicz, « Femtosecond filamentation in air at low pressures. Part II: Laboratory experiments », *Optics Communications*, vol. 261, n° 2, p. 322-326, mai 2006, doi: 10.1016/j.optcom.2005.11.041.
- [10] P. Walch, B. Mahieu, L. Arantchouk, Y.-B. André, A. Mysyrowicz, et A. Houard, « Cumulative air density depletion during high repetition rate filamentation of femtosecond laser pulses: Application to electric discharge triggering », *Applied Physics Letters*, vol. 119, n° 26, p. 264101, déc. 2021, doi: 10.1063/5.0077635.